An investigation on impact-induced oscillations and noise in lubricated conjunctions

An investigation on impact-induced oscillations and noise in lubricated conjunctions

N. Dolatabadi[1], S. Theodossiades[1] and S.J. Rothberg[1]
[1] Wolfson School of Mechanical and Manufacturing Engineering
Loughborough University, Loughborough, LE11 3TU, Leicestershire, UK
e-mail: **n.dolatabadi@lboro.ac.uk**

Abstract
Energy efficiency and Noise, Vibration and Harshness (NVH) have been in the centre of attention for automotive manufacturers during the last decades. Energy losses occur in different forms, such as friction, impacts and noise. Physical understanding of the mechanisms that lead to aggressive dynamics and noise generation is a key in order to design more efficient systems with better NVH performance. In the current study, impact energy is calculated at the lubricated piston-liner conjunctions combining dynamics and tribology. The vibration power at the engine block surface is converted into sound pressure level (SPL) at any desired location analytically. Then, a technique is presented to reduce the severity of impact dynamics by controlling piston's secondary motion, comprising vibration absorbers with nonlinear characteristics. The piston secondary motion dynamics are studied and the absorber effectiveness on vibration reduction is discussed.

1 Introduction

The noise radiated from internal combustion engines can be classified into two main categories: combustion and mechanical noise. The mechanical part comprises various sources, such as piston impacts, bearings, valves, gear contacts etc. Piston impacts in combination with combustion are responsible for about 80% of the overall engine noise [1]. Therefore, the importance of studying piston dynamics is driven by the need for improvements in reducing piston impact severity, engine noise, the associated friction and fuel efficiency. During the conversion of piston reciprocation to crankshaft rotation, side forces are generated on piston pin, which are responsible for piston's secondary motion within the available clearance space. Thus, piston impacts and noise are produced. A comprehensive approach to study piston dynamics in the lubricated conjunctions is by combining tribology and dynamics under a single framework (tribodynamics).

Early studies have neglected the presence of lubricant in the piston-liner conjunctions for reasons of simplicity; therefore, pure structural dynamics were investigated [2]. Generally, piston dynamic analyses either neglect piston rotation about the pin [2-4] or they employ Lagrange's formulation to include the occurring moments due to rotation [5,6]. In later research, the piston-liner contact interactions have been modelled using friction coefficients [7,8]. A more effective method to consider oil-film cushioning effects is by applying Reynolds equation [9-12], where the oil film thickness and its resultant load capacity are calculated at each time step and over the skirt area. When the time history of film thickness is taken into account, the solution is of transient form; otherwise, the approach is deemed as quasi-static. D'Agostino [5] has considered the lubricated conjunctions to be Elasto-hydrodynamic (EHL). In this scenario, the deformations of piston skirt have been considered in the film thickness estimation.

In most piston impact-noise studies, the lubrication conjunctions are replaced by simple spring-damper elements for simplicity of the analysis [6,13]. In the present study, the effects of lubrication and piston skirt deformation have been included in the impact noise calculations. Film-thickness variations can be used to estimate impact attenuation at the inner surface of the cylinder liner. In this way, the transferred

energy to the surface of the engine block is calculated. Having obtained the vibration power on the engine block surface, the sound pressure level (SPL) at any desired distance from the block surface can be estimated. The proposed methodology for the evaluation of impact-noise levels is verified with experimental measurements.

The second part of this study concerns an attempt to control the number and severity of piston impacts. Conventional control methods of piston noise and friction have been presented in the literature by offsetting crankshaft [14,15] and piston-pin [9,16]. In this way, piston is pushed to one side of the cylinder liner for the larger part of crank angle intervals. The piston impact behaviour improves as a result but with an adverse effect on frictional losses. Other studies are dedicated to the modification of piston profile and thickness of the piston skirt [17,18]. A novel approach to control piston impacts is by applying the passive control method of targeted energy transfer (TET), in which a vibration absorber with nonlinear stiffness characteristics and light damping (nonlinear energy sink - NES [19]) is attached to the primary system (here, piston). The NES allows irreversible energy excess transfer from the primary system. Recently, Sigalov et al. [20] have applied TET to a transient strongly nonlinear dynamics problem. The application of a similar approach could be investigated for other fast transient systems, such as piston dynamics. In current work, a pendulum with nonlinear torsional stiffness and linear torsional damping characteristics is attached to piston at the pin location. In order to decrease the complexity of the NES dynamics, piston tribology is simplified to conventional spring-damper elements. A preliminary parametric study is performed to identify mass and stiffness coefficients of the NES for effective TET. The dissipated energy through the absorber is calculated and initial results reveal promising improvements in the severity and number of impacts.

Nomenclature

A_r: area of noise radiating surface

a: distance of pin to the top of piston skirt

b: distance of centre of gravity to the top of piston skirt

COG: piston centre of gravity

c_a: wave speed in air

c_H: damping coefficient of Hertzian contact

c_t: torsional damping coefficient of NES

E_t: dissipated energy through NES damping

E_{tot}: total energy of external excitations

e_b: piston eccentricity at bottom of the skirt

e_t: piston eccentricity at top of the skirt

F_{hyd}: lubrication load on piston skirt

F_s: side force on piston pin

f_G: gas force on top of the piston crown

f_r: reaction force at the four corners of piston skirt

g: gravity

h: oil-film thickness

I_{pis}: piston inertia about the pin

k_H: Hertzian stiffness coefficient

k_t: stiffness coefficient of the NES

L: length (height) of piston skirt

M_{fr}: moment due to f_r

M_{hyd}: moment due to the oil-film reaction force

M_N: torsional moment caused by NES

M_s: moments due to gas force and COG offsets

m_{nes}: mass of NES

m_{pin}: mass of piston pin

m_{pis}: mass of piston

P: oil-film pressure

P_a: acoustic power

P_v: vibration (impact) power

R_n: length of pendulum

t: time

U_{av}: oil average entrainment speed along the liner axis

V_{av}: oil average entrainment velocity perpendicular to the cylinder axis

v: variation of film thickness with time

v_r: vibration velocity of noise radiating surface

x: coordinate along the liner axis

Z: impact impedance

z: coordinate along the piston clearance

β: piston tilt angle

γ: NES angle

δ: piston penetration in the cylinder liner (Hertzian deformation)

η: lubricant dynamic viscosity

η_{tf}: structural transfer function

ρ: lubricant density

ρ_a: density of air

σ: radiation efficiency factor

φ: connecting-rod angle

2 Methodology

The methodology to predict piston impact noise and control the associated dynamics is divided into three areas. The first two (piston tribodynamics and structural attenuation - transfer function) are briefly described below (comprehensively explained in the associated references). The NES model is discussed in more detail.

2.1 Tribodynamics model

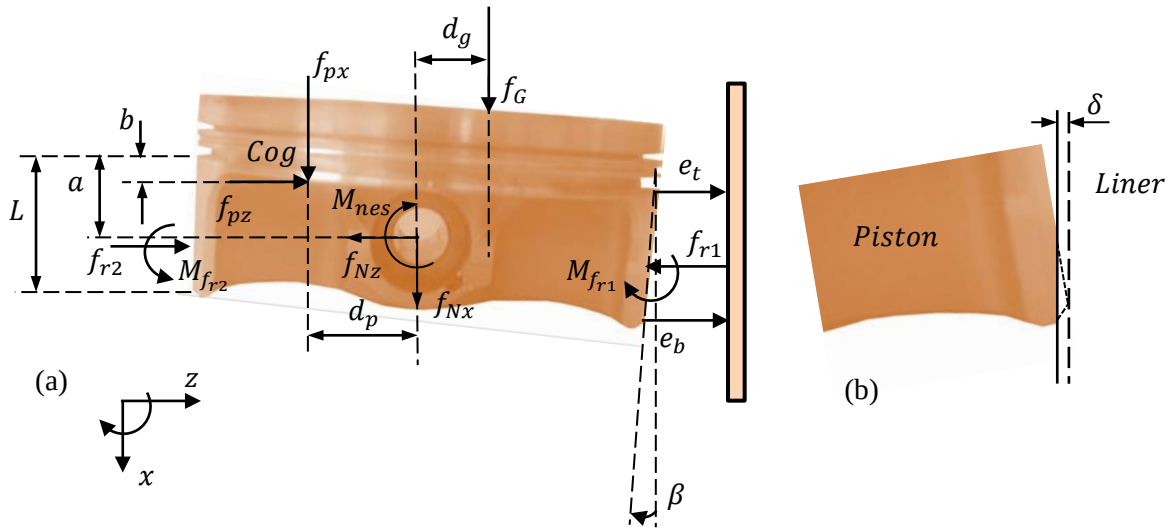

Figure 1: (a) Geometry variable, forces and moments of piston; (b) piston penetration in liner

A piston tribodynamics model has been developed by considering piston translation and rotation (secondary motions). The reaction forces and moments at the lubricated conjunctions are included as external forces in the dynamics and their values are iteratively calculated for each time step (crank angle interval) by solving 2D Reynolds equation. The piston deformation is estimated using the compliance matrix of the skirt and its effect appears in the film thickness predictions. For further details on this model, one can refer to the work of Littlefair [21,22]. Schematic of piston variables, forces and moments are shown in figure 1(a). The equations of motion 1 depict system dynamics in terms of eccentricities e_t and e_b. The oil-film reaction force, F_{hyd}, is obtained from equation 2 (Reynolds transient equation).

$$\begin{bmatrix} m_{pis}\left(1-\frac{b}{L}\right)+m_{pin}\left(1-\frac{a}{L}\right) & m_{pis}\frac{b}{L}+m_{pin}\frac{a}{L} \\ \frac{I_{pis}}{L}+m_{pis}(a-b)\left(1-\frac{a}{L}\right) & -\frac{I_{pis}}{L}+m_{pis}(a-b)\frac{b}{L} \end{bmatrix} \begin{Bmatrix} \ddot{e}_t \\ \ddot{e}_b \end{Bmatrix} = \begin{Bmatrix} F_{hyd}+F_s \\ M_{hyd}+M_s \end{Bmatrix} \quad (1)$$

$$\frac{\partial}{\partial x}\left(\frac{\rho h^3}{\eta}\frac{\partial P}{\partial x}\right)+\frac{\partial}{\partial z}\left(\frac{\rho h^3}{\eta}\frac{\partial P}{\partial z}\right)=12\left\{U_{av}\frac{\partial}{\partial x}(\rho h)+V_{av}\frac{\partial}{\partial z}(\rho h)+\frac{d}{dt}(\rho h)\right\} \quad (2)$$

2.2 Structural transfer function

Transfer functions are usually derived empirically in the literature. The work of Ungar and Ross studies this derivation theoretically [2], where the term structural attenuation factor is employed. The same idea is used in this paper, except the fact that vibration power and impact impedance are estimated from Reynolds equation rather than explicitly from piston dynamics. Vibration power is the ratio of impact energy over time, evaluated between two successive time steps, as indicated in equation 3:

$$P_v=\frac{\int_{t_1}^{t_2}\bar{F}_{hyd}v dt}{dt}=\frac{\int_{t_1}^{t_2}Zv^2 dt}{dt} \quad (3)$$

Here, $\bar{F}_{hyd}$ is the average oil film load capacity between two consecutive time steps, v is the film thickness variation rate and dt is the time between the mentioned time steps. Impact impedance (Z) is the ratio of load capacity over film velocity, calculated from Reynolds equation at each time step:

$$Z=\frac{F_{hyd}}{v} \quad (4)$$

Having predicted the vibration (impact) power, the acoustic power is required to determine the transfer function. The acoustic power is related to the air characteristics and vibration velocity of the engine block. With impact velocity, v, known from Reynolds equation, the radiation velocity, v_r, is obtained using conservation of energy. The acoustic power is then calculated as:

$$P_a=\sigma\rho_a c_a A_r v_r^2 \quad (5)$$

According to Ungar and Ross [2], the structural transfer function is given by:

$$\eta_{tf}=\frac{P_a}{P_v} \quad (6)$$

Having calculated the acoustic power at the engine block surface, the estimation of sound pressure level (SPL) near the block or at any desired location is now possible.

2.3 NES model

It is assumed that the proposed pendulum model for the NES comprises a point mass at the end of a bar with negligible mass. The other end communicates with piston through nonlinear torsional stiffness and weak linear viscous damper. This spring-damper arrangement allows the NES to dissipate energy effectively from the primary system under certain operating conditions and system properties with the stiffness nonlinearity enabling NES to cover a wider range of impact frequencies. The pendulum model is shown in figure 2.

Considering the proposed model in figure 2, the equations of motion are reproduced to include the NES contribution and the inertial matrix of the system is given by:

$$\begin{bmatrix} m_{pis}\left(1-\frac{b}{L}\right)+\left(m_{pin}+m_{nes}\right)\left(1-\frac{a}{L}\right) & m_{pis}\frac{b}{L}+\left(m_{pin}+m_{nes}\right)\frac{a}{L} & -m_{nes}R_n(\cos\gamma+\sin\gamma\tan\varphi) \\ \frac{I_{pis}}{L}+m_{pis}(a-b)\left(1-\frac{a}{L}\right) & -\frac{I_{pis}}{L}+m_{pis}(a-b)\frac{b}{L} & 0 \\ -m_{nes}R_n\left(1-\frac{a}{L}\right)\cos\gamma & -m_{nes}R_n\frac{a}{L}\cos\gamma & m_{nes}R_n^2 \end{bmatrix} \quad (7)$$

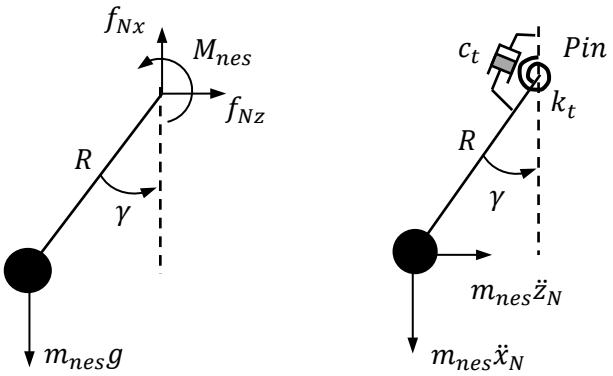

Figure 2: Schematic of the NES attachment

As already mentioned, the lubricated conjunction has been replaced by a spring-damper model for reduction of the computation time. The damping coefficient is obtained by applying the Caughey method through the linearised system [23]. The stiffness coefficient is that of Hertzian point contacts [24]. Four spring-damper arrangements are located at the piston skirt corners. The resultant reactions are activated whenever piston penetrates the cylinder liner ($\delta \geq 0$). Variable δ is depicted in figure 1(b).

$$f_r = \pm k_H \delta^{\frac{3}{2}} - c_H \dot{\delta}, \qquad \delta \geq 0 \tag{8}$$

The sign of stiffness term is determined based on the direction of piston deflection (penetration is an amplitude variable). Knowing the reactions, the vector of external forces and moments is produced as:

$$\begin{Bmatrix} \left(-f_G + \left(m_{pin} + m_{pis} + m_{nes}\right)\ddot{x} - m_{nes}R_n\dot{\gamma}^2\cos\gamma - m_{nes}g\right)\tan\varphi - m_{nes}R_n\dot{\gamma}^2\sin\gamma + \sum f_{ri} \\ M_{nes} + \sum M_{f_r,i} \\ -M_{nes} - m_{nes}R_n g\sin\gamma + m_{nes}R_n\ddot{x}\sin\gamma \end{Bmatrix} \tag{9}$$

M_{nes} is the moment created by the nonlinear torsional stiffness and linear torsional damper:

$$M_{nes} = k_t(\gamma - \beta)^3 + c_t\left(\dot{\gamma} - \dot{\beta}\right) \tag{10}$$

These equations are iteratively solved using a Newmark integration scheme for nonlinear equations [25]. The output of this solution is evaluated by calculating the percentage of dissipated energy from the primary system during the entire engine cycle through viscous damping action. The dissipated energy is the numerator of equation 11 while the denominator shows the total energy of external excitations (gas force), which is calculated using equation 12.

$$E_t\% = \frac{\int c_t\left[\dot{\gamma} - \dot{\beta}\right]^2 dt}{E_{tot}} \times 100 \tag{11}$$

$$E_{tot} = \int f_G(t)\dot{x}dt \tag{12}$$

3 Results and discussion

3.1 Noise SPL

The results discussed in this section are a combined outcome of piston tribodynamics and structural transfer function analysis. Using the output of these models, the acoustic power is obtained and sound pressure levels (SPL) are evaluated at 1 m distance from the engine block (4250rpm crankshaft speed). Noise experimental measurements are recorded at the same location. The experiment is performed on a Honda CRF 450R single-cylinder, 4-stroke SI engine. A comparison between the numerical and experimental results is shown in figure 3. There is generally reasonable agreement between experiment and numerical calculations, although the latter overestimates SPL during combustion. It is noted that the proposed noise methodology is applicable for the estimation of engine noise due to piston impacts.

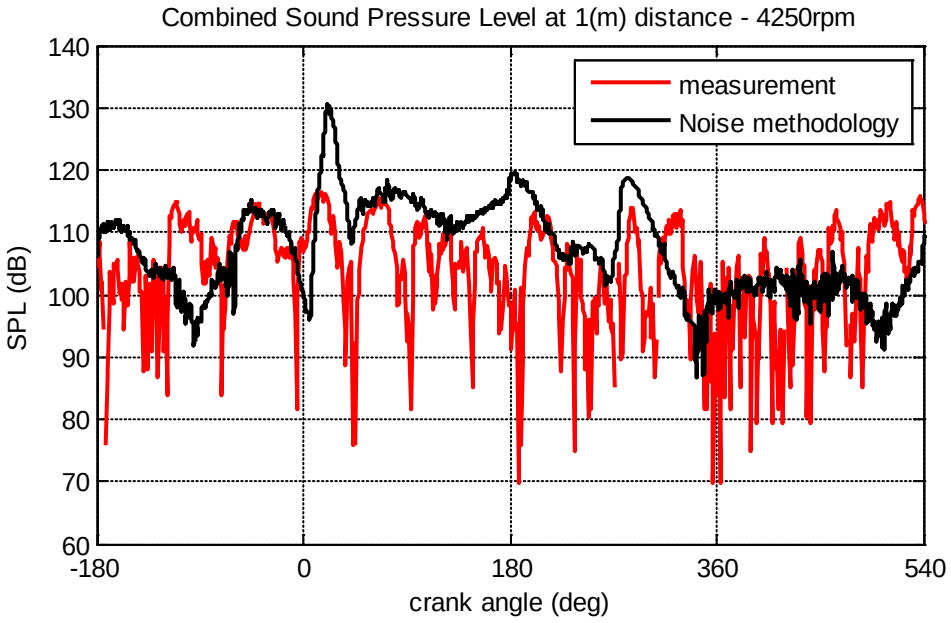

Figure 3: Numerically and experimentally obtained SPL of piston-impact noise

3.2 NES simulation

For NES simulations, the torsional damping coefficient, c_t, is set as constant and equals 0.01. The NES stiffness varies from 4 to 1000 Nm/rad with its mass varying from 10% to 20% of the piston mass. The pendulum length is fixed, arbitrarily chosen to be 5 cm. The energy dissipated by the NES is recorded. The results of this study are presented in figure 4. Each curve corresponds to a different value of the NES/piston mass ratio. The results are presented in logarithmic scales. As it can be seen, the dissipated energy increases with mass ratio regardless of the stiffness coefficient value. For each mass ratio, increase of stiffness coefficient results in weaker energy dissipation. The highest percentage of energy consumed (6%) occurs for NES mass ratio of 20% and stiffness of 4 Nm/rad. Lower stiffness coefficients have better effects on energy dissipation, but it may not be efficient to introduce these due to impact severity and NES motion constraints.

The ideal vibration absorber is the one that dissipates maximum energy and at the same time it reduces the number and severity of impacts. Thus, a criterion to study the nature of impacts during engine cycle is introduced. Two ways to approach piston impacts have been used (figure 5), based on the conventional method of identifying the occurring side force. In the first one, the values of primary forces are considered. When the gas force (blue curve) intersects with inertia force (black curve), the two forces are

equal in the primary direction. In this instance, piston can start moving within the clearance, depending on the force values before and after equality. The second approach depends entirely on piston tribodynamics and the side force is calculated using reaction forces from Reynolds solution. The occurrence of impact is identified when the side force changes sign (red curve in figure 5). There are some flaws in these methods. Initially, comparison between the two approaches shows that there are some phase differences between their predictions. Moreover, the first approach (equality of forces) anticipates two impacts less than the second approach (side force sign). Additionally, the side force is acting on piston pin, which presents pure translation within its clearance and the effect of piston rotation on the impacts' number and severity is neglected. Due to piston rotation, the number of impacts at top and bottom of the skirt might be different from that at the piston-pin location.

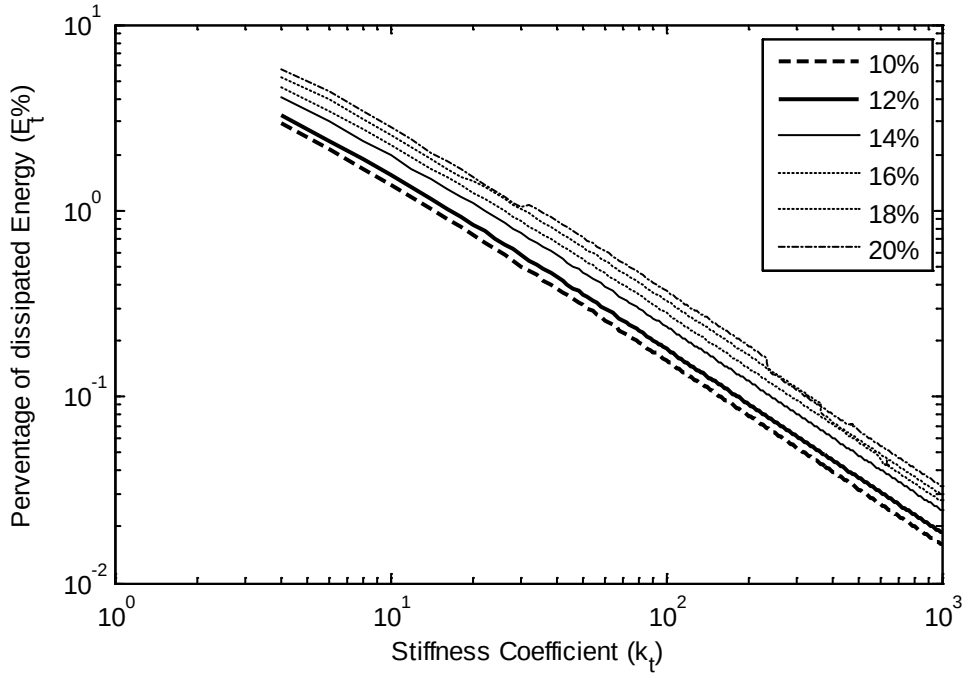

Figure 4: Variation of NES dissipated energy with stiffness coefficient and NES/piston mass ratio

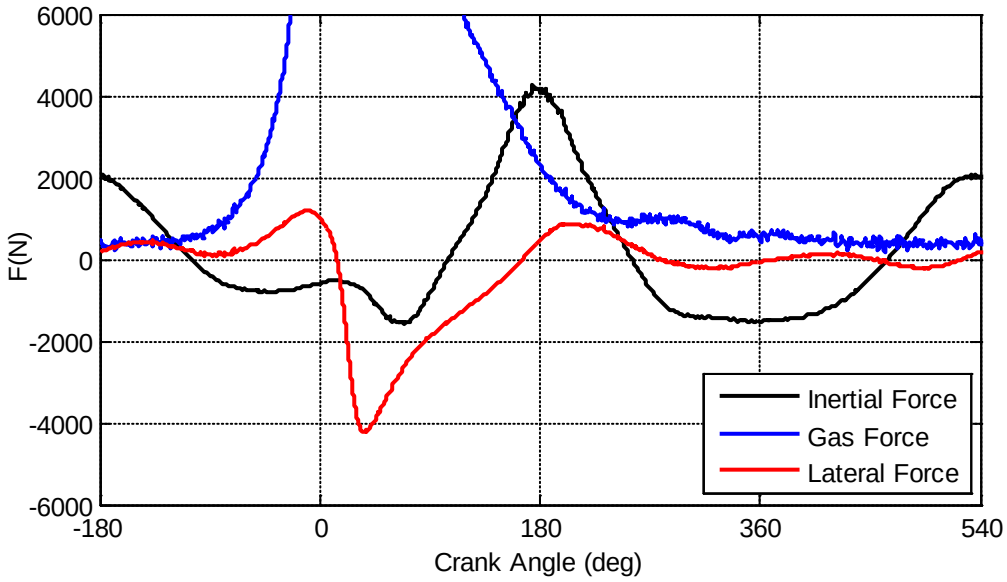

Figure 5: Graphical representation of piston impact identification

For the aforementioned reasons, a slightly different approach has been used in this study. Piston eccentricities at top and bottom of the skirt are used to determine the number of potential impacts. Piston rotation effects are already embedded in this method as eccentricities are functions of piston translation/rotation. As piston eccentricity changes sign (crossing the centre line of the cylinder liner), impact occurrence is possible. This condition is applied and impacts are recorded separately at the top and bottom of the skirt. The resulting data are presented in figures 6 and 7, which refer to top and bottom eccentricity, respectively. The stiffness coefficient is limited to 100 Nm/rad in these graphs for clearer illustration, since better results are observed in this region. The number of possible impacts varies from 4 to 11 at top eccentricity. The smallest number of possible events (4 impacts) occurs for $k_t < 10$ Nm/rad and mass ratio 20% (brown line).

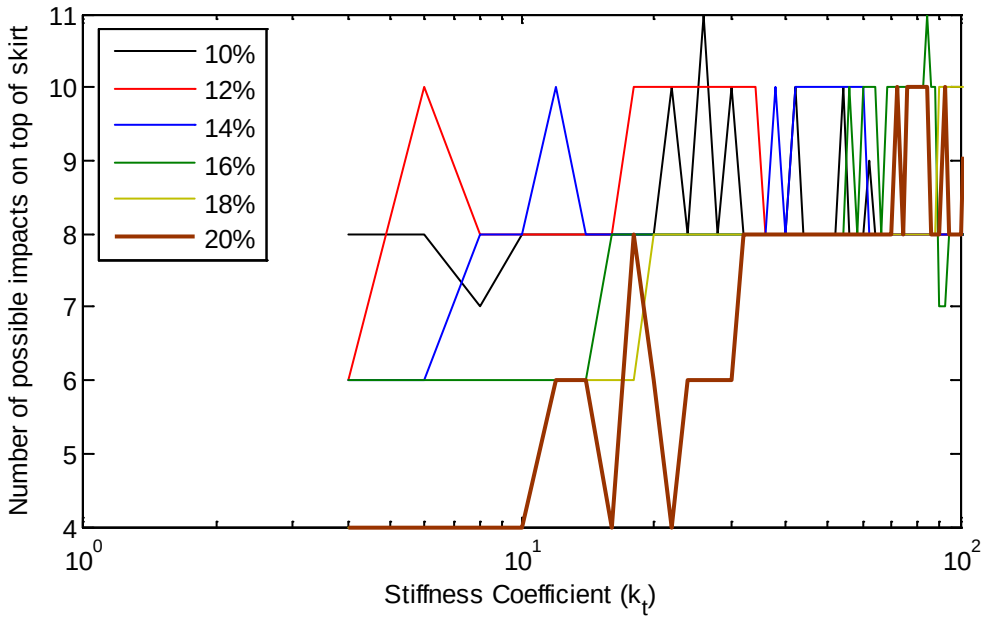

Figure 6: Number of potential impacts at the top of piston skirt for different NES stiffness coefficients and mass ratios

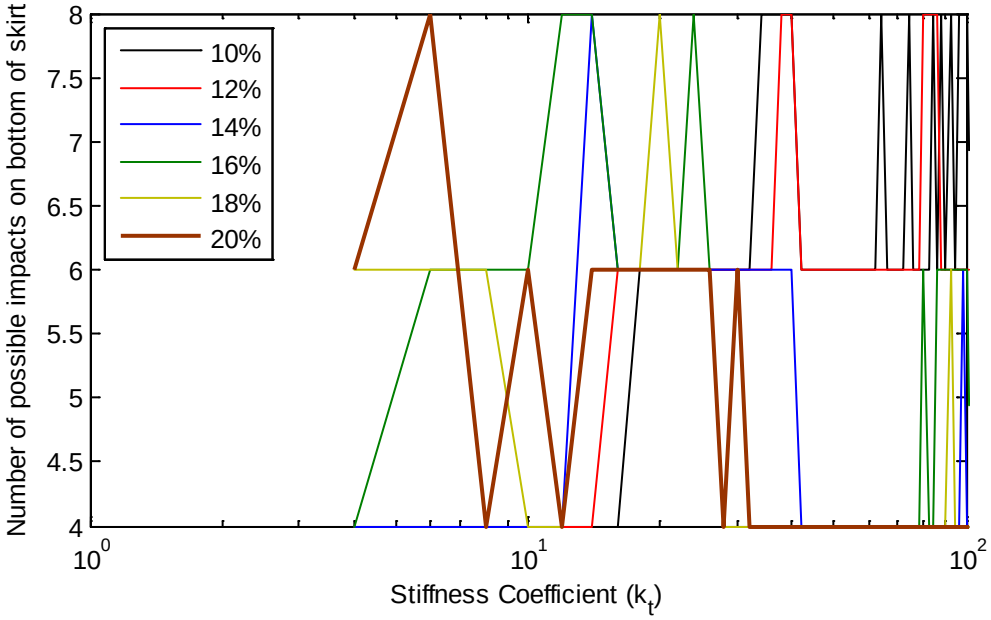

Figure 7: Number of potential impacts at the bottom of piston skirt for different NES stiffness coefficients and mass ratios

Similar analysis for bottom eccentricity reveals that the number of impacts is at its minimum for a large stiffness coefficient interval and even mass ratio of 14%. However, mass ratio of 20% is more beneficial, since energy dissipation is higher for this value (brown curve). Moreover, the number of impacts on the skirt top is small at this ratio as well. The smallest stiffness coefficient where the number of impacts is 4 for this mass ratio is $k_t = 8$ Nm/rad. Thus, the combination of $k_t = 8$ Nm/rad and mass ratio of 20% will be used thereafter in this study. This combination results in energy dissipation of over 3%. In this scenario, the number of impacts at the top and bottom of the skirt are equal. A review of other combinations of NES characteristics proves that the number of impacts at the top and bottom of the skirt is different and application of the side force criterion is not sufficient, as it predicts a single number of impacts and neglects piston rotation.

To visualise the NES effectiveness, a comparison is shown between results of system dynamics with and without NES. Two sets of data are important: (i) eccentricity acceleration and (ii) eccentricity. The former is indicative of piston inertial forces at top and bottom, which influence impact severity. Eccentricity values show the position of piston within the clearance area, revealing the number of impacts. In this study, the model simulation was run for 60 engine cycles to let the system reach steady state conditions. The last four cycles have been plotted.

Figure 8 depicts eccentricity accelerations at top and bottom of the skirt. In all graphs, black/red curves correspond to piston dynamics without/with NES. At the skirt top and bottom, combustion appears in the form of bigger spikes. In general, accelerations are larger at the bottom of the skirt without the NES. NES seems to have less influence on the top eccentricity acceleration. In some areas, it even increases its amplitude; however, this growth is not remarkable in comparison to the improvement noticed in the bottom eccentricity acceleration, which is nominally almost twice the top acceleration amplitude. The combustion spike at the bottom eccentricity acceleration shows that NES has reduced the amplitude to less than the half of the initial value. This reduction is also observed in few other locations of the engine cycle. It is also noted that some phase differences have appeared between similar spikes in the two cases. As an average, the spike amplitudes in the whole cycle have reduced remarkably.

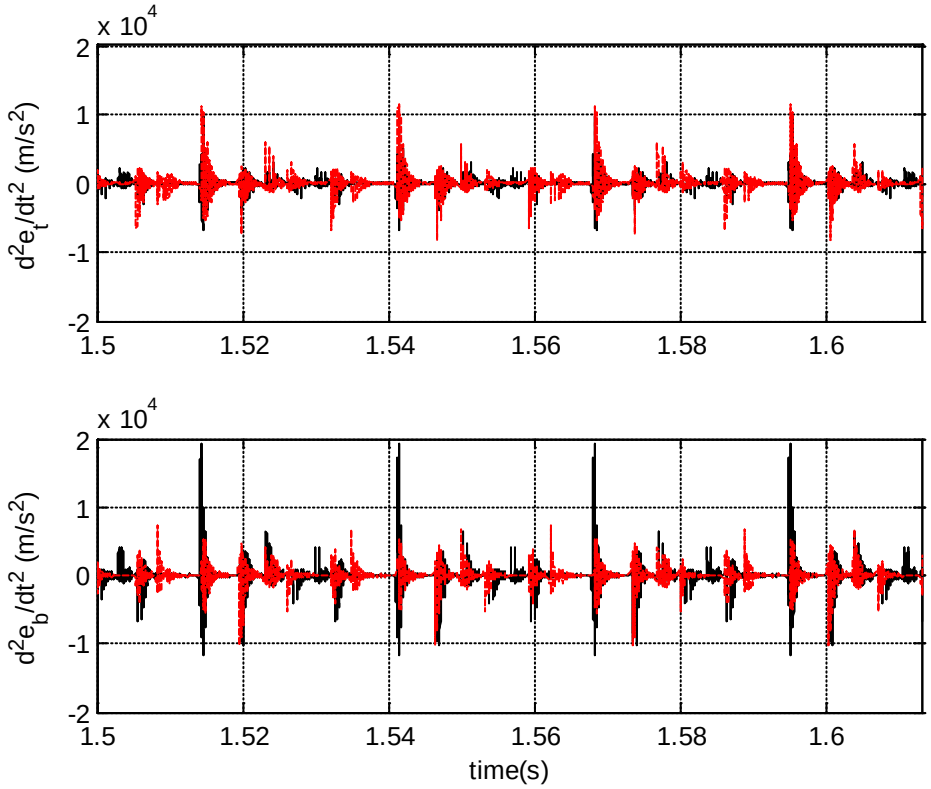

Figure 8: Eccentricity acceleration at piston top (top graph) and bottom (bottom graph) locations for systems with (red curve) and without (black curve) NES.

Eccentricity graphs are shown in figure 9, revealing a reduction on impact severity. The piston trajectory also shows the number of impacts as piston moves from one side of the cylinder liner to the opposite. The top graph depicts the eccentricity at the top of the skirt, where piston displacement is slightly larger. However, two piston translations are eliminated between 1.52s and 1.54s (meaning that two piston impacts are removed). At the bottom of the skirt, the same number of impacts is eliminated due to the NES action. As it is shown in the NES equipped system, the bottom of the skirt remains at the thrust side (negative eccentricity) during combustion. The top eccentricity changes direction, inducing one impact. After 1.52s, the top of the skirt moves to thrust-side and remains there almost up to 1.53s. The bottom of the skirt alters between thrust- and anti-thrust sides and remains at the anti-thrust side. The third graph shows piston-pin translation. It is clearly seen that the pin remains close to the cylinder's centre line before combustion while during combustion it stays at the thrust-side wall, meaning that piston tilts before combustion with tilt angle being zero during combustion. The same observation applies to piston-pin translation around 1.53s (anti-thrust side). 4 impacts are observed in the trajectories of figure 9. This may not be the case though for different combinations of NES stiffness and mass ratio, as discussed earlier.

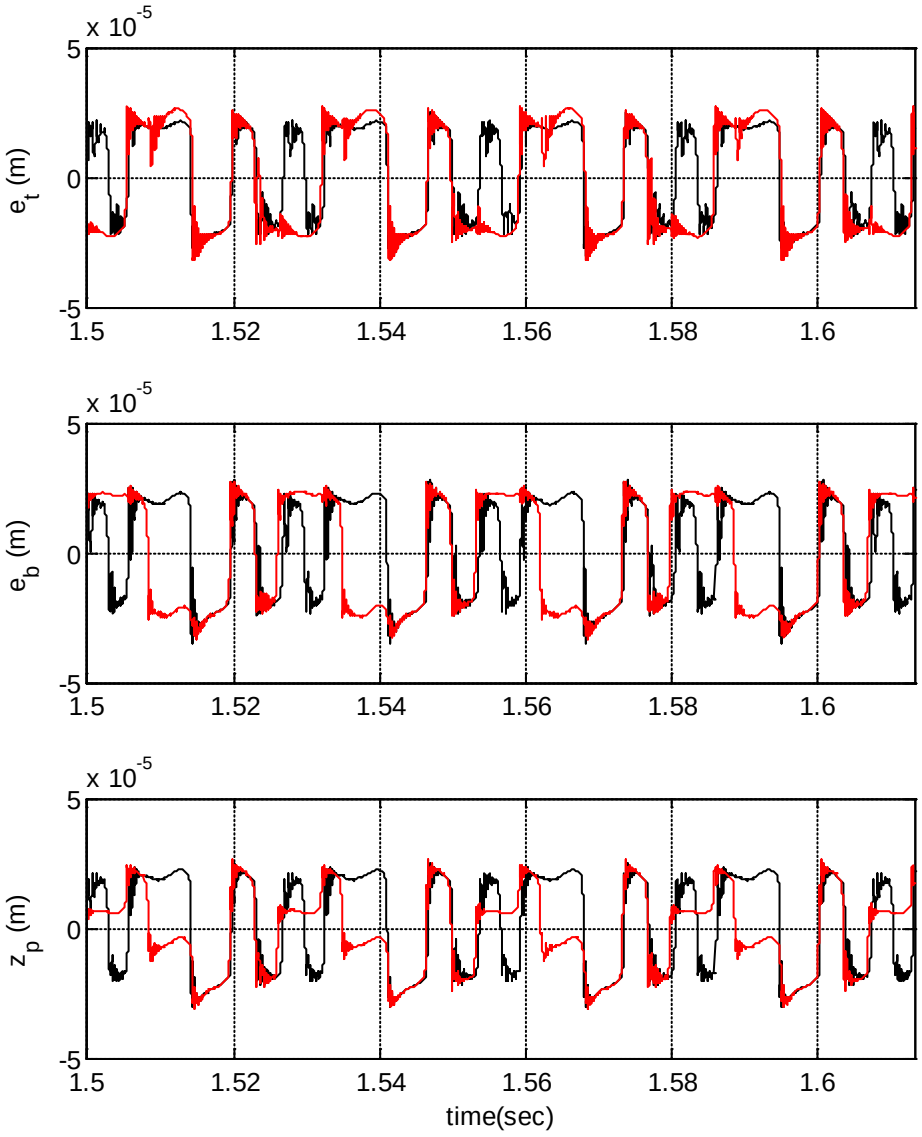

Figure 9: Eccentricity at piston top (top graph) and bottom (bottom graph) locations for systems with (red curve) and without (black curve) NES.

4 Conclusions

A methodology to quantify noise levels due to piston impacts and control piston dynamics has been presented in this paper. The proposed method is validated against experimental noise measurements, showing that combination of lubricated conjunctions, piston secondary motion and skirt deformation under a single framework can determine piston mechanical noise. According to literature, piston impact noise is comparable to the overall engine noise levels; therefore, a novel method to control the number and severity of piston impacts is proposed based on the use of vibration absorbers with nonlinear characteristics. A preliminary parametric study reveals that small stiffness coefficients and larger NES mass ratios lead to higher energy dissipation at the absorber. The other design parameter is the minimum number of piston impacts, which - as shown - is different for the top and bottom of the piston skirt. Therefore, it is important to consider piston rotation when studying its secondary dynamics. It has been shown that the conventional methods for this purpose are not sufficiently capturing the number of impacts, as they only consider piston translation by taking the side force into account. The combination of dissipated energy in the NES and minimum number of impacts leads to the optimum NES design. The presentation of piston eccentricity acceleration and displacement shows that the application of NES is beneficial in the reduction of piston impacts, especially in the combustion stroke (where maximum impact force occurs). As future work, the NES characteristics should be determined more accurately for engine speed operating conditions applicable to the single cylinder engine under investigation.

Acknowledgements

The authors wish to express their gratitude to the EPSRC for the financial support extended to the Encyclopaedic Program Grant, under which this research was carried out.

References

[1] H. Kanda, M. Okubo, T. Yonezawa, *Analysis of noise sources and their transfer paths in diesel engines,* SAE Technical Paper, No. 900014, SAE (1990), pp. 1-8.

[2] E.E. Ungar, D. Ross, *Vibrations and noise due to piston-slap in reciprocating machinery,* Journal of Sound and Vibration, Vol. 2, No. 2, Elsevier (1965), pp. 132-146.

[3] N. Lalor, E. Grover, T. Priede,*Engine noise due to mechanical impacts at pistons and bearings,* Society of Automotive Engineers, (1980).

[4] V.I. Zinchenko, *Noise of marine diesel engines,* Sudpromgiz (1952).

[5] V. D' Agostino, D. Guida, A. Ruggiero, C. Russo. *Optimized EHL piston dynamics computer code,*in Anonymous , editor(s) *Proceedings of the 5th International Tribology Conference, AITC-AIT,* (2006), pp. 9.

[6] S.H. Cho, S.T. Ahn, Y.H. Kim, *A simple model to estimate the impact force induced by piston slap,* Journal of Sound and Vibration, Vol. 255, No. 2, Elsevier (2002), pp. 229-242.

[7] S. Haddad, D. Howard, *Analysis of piston slap-induced noise and assessment of some methods of control in diesel engines,* SAE Technical Paper, No. 800517, SAE (1980), pp. 1-12.

[8] R. Wilson, J. Fawcett, *Dynamics of the slider-crank mechanism with clearance in the sliding bearing,* Mechanism and Machine Theory, Vol. 9, No. 1, Elsevier (1974), pp. 61-80.

[9] T. Nakada, A. Yamamoto, T. Abe, *A numerical approach for piston secondary motion analysis and its application to the piston related noise,* SAE paper, No. 972043, SAE (1997), pp. 1361-1370.

[10] F. McClure, *Numerical modeling of piston secondary motion and skirt lubrication in internal combustion engines,* PhD, Massachusetts Institute of Technology, United States of America (2007).

[11] J. Cho, S. Moon, *A numerical analysis of the interaction between the piston oil film and the component deformation in a reciprocating compressor,* Tribology International, Vol. 38, No. 5, Elsevier (2005), pp. 459-468.

[12] M. Perera, S. Theodossiades, H. Rahnejat, *A multi-physics multi-scale approach in engine design analysis,* Proceedings of the Institution of Mechanical Engineers, Part K: Journal of Multi-body Dynamics, Vol. 221, No. 3, Sage Publications (2007), pp. 335-348.

[13] K. OHTA, K. AMANO, A. HAYASHIDA, G. ZHENG, *Analysis of Piston Slap Induced Noise and Vibration of Internal Combustion Engine,* Journal of Environment and Engineering, Vol. 6, No. 3, J-STAGE (2011), pp. 712-722.

[14] M. Perera, S. Theodossiades, H. Rahnejat, *Elasto-multi-body dynamics of internal combustion engines with tribological conjunctions,* Proceedings of the Institution of Mechanical Engineers, Part K: Journal of Multi-body Dynamics, Vol. 224, No. 3, Sage Publications (2010), pp. 261-277.

[15] K. Nakayama, S. Tamaki, H. Miki, M. Takiguchi, *The Effect of Crankshaft Offset on Piston Friction Force in a Gasoline Engine,* SAE Technical Paper, Vol. SP-1495, No. 2000-01-0922, SAE International(2000), pp. 1-8.

[16] K. Nakashima, Y. Yajima, K. Suzuki, *Approach to minimization of piston slap force for noise reduction–investigation of piston slap force by numerical simulation,* JSAE Review, Vol. 20, No. 2, Elsevier (1999), pp. 211-216.

[17] R. Keribar, Z. Dursunkaya, *A comprehensive model of piston skirt lubrication,* SP-919, Engine Tribology, SAE Paper, Vol. 920483, SAE (1992), pp. 11-19.

[18] J. CHO, *Effects of skirt profiles on the piston secondary movements by the lubrication behaviors,* International journal of automotive technology, Vol. 5, No. 1, 한국자동차공학회 (2004), pp. 23-31.

[19] Y. Lee, A.F. Vakakis, L. Bergman, D. McFarland, *Passive non-linear targeted energy transfer and its applications to vibration absorption: a review,* Proceedings of the Institution of Mechanical Engineers, Part K: Journal of Multi-body Dynamics, Vol. 222, No. 2, SAGE Publications (2008), pp. 77-134.

[20] G. Sigalov, O. Gendelman, M. Al-Shudeifat, L. Manevitch, *Resonance captures and targeted energy transfers in an inertially-coupled rotational nonlinear energy sink,* Nonlinear Dynamics, Vol. 69, No. 4, Springer (2012), pp. 1693-1704.

[21] B. Littlefair, *A Tribo-dynamic solution for the flexible piston skirt and liner conjunction,* PhD, Wolfson School of Mechanical and Manufacturing Engineering, Loughborough University, United Kingdom (2013).

[22] B. Littlefair, M. De la Cruz, S. Theodossiades, R. Mills, *Transient Tribo-Dynamics of Thermo-Elastic Compliant High-Performance Piston Skirts,* Tribology Letters, Springer (2013), pp. 1-20.

[23] T. Caughey, M. O'kelly, *Classical normal modes in damped linear dynamic systems,* Journal of Applied Mechanics, Vol. 32, No. 3, American Society of Mechanical Engineers (1965), pp. 583-588.

[24] H. Hertz, *On the contact of elastic solids,* J.reine angew.Math, Vol. 92, No. 156-171, (1881), pp. 110.

[25] S. Timoshenko,*Vibration problems in engineering,* John Wiley and Sons, United States of America (1974).